PAPER

Check for updates

Direct inhibition of Keap1–Nrf2 interaction by egg-derived peptides DKK and DDW revealed by molecular docking and fluorescence polarization†

Liangyu Li, [ID][a] Jingbo Liu,[a] Shaoping Nie,[b] Long Ding,[a] Liying Wang,[a] Jiyun Liu,[a] Wenchao Liu[a] and Ting Zhang [ID] *[a]

Egg-derived small peptides have various biological activities, including antioxidant properties. The Keap1–Nrf2 pathway is central to cell resistance to oxidative stress. In this study, we screened an egg-derived short peptide library to identify molecules with a potential to directly inhibit the Keap1–Nrf2 interaction, using molecular docking, fluorescence polarization assay, and a cytotoxicity model. Among the 20 small peptides selected by molecular docking, two tri-peptides, DKK and DDW, could directly inhibit the binding of the Keap1 Kelch domain to the FITC-labelled 9-mer Nrf2 peptide, as evidenced by increased K_d in fluorescence polarization experiments. Furthermore, in H_2O_2-treated cells, DKK and DDW promoted survival and upregulated the activity of catalase and superoxide dismutase, key enzymes involved in detoxification of reactive oxygen species. Our findings indicate that small egg-derived peptides DKK and DDW can exert antioxidant effects and protect cells against oxidative stress by directly inhibiting Keap1–Nrf2 interaction.

1. Introduction

Eggs are an excellent source of dietary proteins, such as egg white proteins, which are easier to digest and absorb than other food-derived proteins such as those from chicken, beef, and milk. Egg proteins are rich in amino acids, including eight essential and 12 nonessential amino acids, which are the building blocks of the majority of proteins in living organisms. Furthermore, the peptides produced as a result of egg protein degradation are suggested to have additional biological activities compared to the whole-egg proteins and have become a target of extensive research on foodborne bioactive peptides.[1–3] One of the most important biological properties of egg-derived peptides is their antioxidant activity.[4–6] However, very often egg peptides demonstrating antioxidant activity in chemical experiments fail to do so in cell cultures and animal models, and the reason is generally acknowledged to be peptide degradation, which accounts for the rapid drop of the activity of egg-derived peptides after they enter the cell. In this respect, the use of short peptides consisting of two or three amino acids can provide a solution to this problem because these peptides can

be completely absorbed in the small intestine and their activity will not be affected during the process.[7,8]

Studies on antioxidant peptides are focused on the molecular mechanisms underlying their biological activity.[9] The Keap1–Nrf2 pathway is the most important regulator of cytoprotective responses to oxidative stress caused by various exogenous and endogenous factors.[10,11] The main players in this signalling mechanism are transcription factor Nrf2 (nuclear factor erythroid 2-related factor 2) and repressor protein Keap1 (Kelch-like ECH-associated protein 1) which promotes Nrf2 proteasomal degradation.[12] Under basal conditions, Keap1 forms a homodimer through BTB domains and then binds to DLG and ETGE motifs of the Neh2 domain in Nrf2 via two Kelch domains, resulting in Nrf2 ubiquitylation and degradation.[10,13–15] When cells are exposed to oxidative stress, cysteine residues in the Keap1 BTB and IVR domains are modified, leading to conformational changes in the Keap1 homodimer and dissociation of the Nrf2 inhibitory complex, which prevents Nrf2 degradation.[16,17] As a result, the accumulated Nrf2 translocates to the nucleus and activates gene expression of a series of phase II detoxification enzymes, including hemeoxygenase 1 (HO-1), NAD(P)H dehydrogenase 1 (NQO1), superoxide dismutase (SOD), and catalase (CAT), involved in antioxidative mechanisms and cell protection from oxidative stress.[17,18]

On the basis of these data, it can be hypothesized that external molecules that can promote the dissociation of the Keap1–Nrf2 complex and increase intracellular Nrf2 accumulation would enhance cell resistance to oxidative stress and, consequently, improve the health status of the organism.[10,19]

[a]Jilin Key Laboratory of Nutrition and Functional Food, Jilin University, Changchun 130062, People's Republic of China. E-mail: tingzhang@jlu.edu.cn; Tel: +86 431 87836351

[b]State Key Laboratory Food Science & Technology, Nanchang University, Nanchang 330047, People's Republic of China

† Electronic supplementary information (ESI) available. See DOI: 10.1039/c7ra04352j
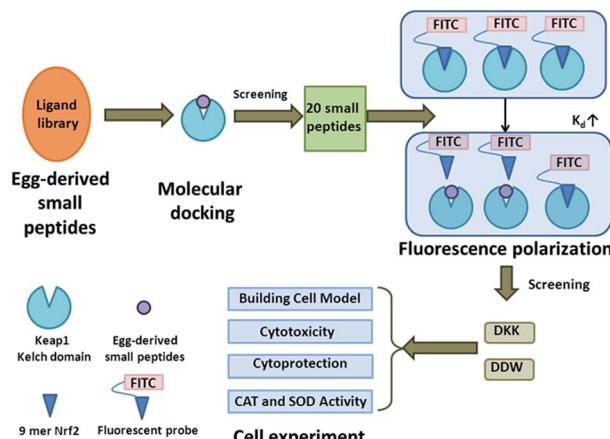
Fig. 1 Schematic illustration of the experimental design of the study.

2.2. Docking experiments

To test docking interactions, we followed the method of Onoda et al.[22] with some modifications. The ligand library comprised 400 di-peptides and 6138 tri-peptides generated by degradation of egg proteins (Tables 1 and S1†), including egg white and egg yolk proteins, and proteins of fertilized eggs. The sequences of these proteins were obtained from the Uniport database (http://www.uniprot.org). Then, the ligand library was analysed using Merck Molecular Force Field, and energy minimization was applied to the calculation. Among the 24 PDB files (Table 2) relevant to human Keap1 protein and found in the RCSB database (http://www.pdb.org), only 13 contained ligands and could

Such antioxidant molecules, known as Keap1–Nrf2 interaction inhibitors, can exert indirect and direct effects. Indirect inhibitors modify the conformation of the key cysteine residues in the Keap1 BTB and IVR domains, whereas direct inhibitors bind to the Kelch domain of Keap1 and occupy the Keap1–Nrf2 binding site. The result of both reactions is the inhibition of Keap1–Nrf2 interaction and activation of the pathway.[20] However, the indirect inhibitors may promote side effects, as they can also modify cysteine residues of other cell proteins and affect their normal functional activity.[10] Therefore, the direct inhibitors have higher specificity and are potentially less toxic compared to the indirect ones, and, thus, are more physiologically suitable for use in humans.[10,21]

The objective of this study was to screen natural egg-derived antioxidant peptides for direct inhibition of the Keap1–Nrf2 interaction (Fig. 1).

2. Materials and methods

2.1. Materials and chemicals

Di-peptides (EK, DW, WE, EY, DK, and EW), tri-peptides (DKE, EWE, EEW, EDW, DWE, DKD, QKE, ECD, DET, DKQ, DWD, DEW, DKK, and DDW), the 9-mer Nrf2 peptide (H-LDEETGEFL-OH, residues 76–84), and a fluorescent probe (FITC-conjugated 9-mer Nrf2 peptide) were purchased from Shanghai Qiang Yao Biological Technology Co., Ltd (Shanghai, China, http://www.chinapeptides.com). The Kelch domain of the human Keap1 (residues 321–609) was purchased from Nanjing Zoonbio Biotechnology Co., Ltd (Nanjing, China). HepG2 cells were obtained from Chinese Infrastructure of Cell Line Resources. Dulbecco's modified Eagle's medium (DMEM), foetal bovine serum (FBS), penicillin–streptomycin solution, and MEM Nonessential Amino Acids were obtained from Gibco (USA). The Cell Titer 96® AQueous One Solution Cell Proliferation kit (MTS assay) was purchased from Promega Biotechnology Co. Ltd (Beijing, China). Bicinchoninic acid assay (BCA) and SOD and CAT assay kits were purchased from Nanjing Jiancheng Bioengineering Co. (Nanjing, China). Cell lysis buffer was purchased from Beyotime Institute of Biotechnology (Shanghai, China).

Table 1 Protein sources of the ligand library

Uniprot ID	Protein	Length (aa)
P01012	Ovalbumin	386
P01013	Ovalbumin-related protein X	232
P01014	Ovalbumin-related protein Y	388
I0J178	Ovalbumin-related protein Y	388
I0J179	Ovalbumin-related protein Y	388
P02789	Ovotransferrin	705
F1NVN3	Ovotransferrin	738
Q4ADJ7	Ovotransferrin	705
Q4ADG4	Ovotransferrin	705
Q4ADJ6	Ovotransferrin	705
E1BQC2	Ovotransferrin	707
Q92062	Ovotransferrin	738
E1BVL8	Ovotransferrin	731
P01005	Ovomucoid	210
B6V1G0	Ovomucoid	210
I0J170	Ovoglobulin G2	439
I0J171	Ovoglobulin G2	439
I0J172	OvoglobulinG2 type AA	439
I0J173	OvoglobulinG2 type AB	439
I0J174	OvoglobulinG2 type AB	439
I0J175	OvoglobulinG2 type BB	439
Q98UI9	Mucin-5B	2108
F1NBL0	Mucin-6	1185
P00698	Lysozyme C	147
P10184	Ovoinhibitor	472
Q9PSS0	Ovomacroglobulin	208
P02701	Avidin	152
P01038	Cystatin	139
E1BYI2	Cystatin	147
R4GLT1	Cystatin	139
P87498	Vitellogenin-1	1912
P02845	Vitellogenin-2	1850
Q91025	Vitellogenin-3	347
O57579	AminopeptidaseEy	972
P02752	Riboflavin-binding protein	283
P05094	Alpha-actinin-1	893
P41263	Retinol-binding protein 4	196
Q5ZIM6	Protein AATF	574
Q6IV20	Gallinacin-11	104
Q8AXU9	Endophilin-A3	353
P27731	Transthyretin	150
Q91044	NT-3 growth factor receptor	827
P19121	Serum albumin	615
O57604	Podocalyxin	571
P02659	Apovitellenin-1	106
Q05744	Cathepsin D	398

Table 2 PDB files of the human Keap1 protein in the RCSB database

Index	PDB ID	Resolution (Å)	Index	PDB ID	Resolution (Å)
1	1U6D	1.85	13	4IFN	2.40
2	1ZGK	1.35	14	4IN4	2.59
3	2FLU	1.50	15	4IQK	1.97
4	3VNG	2.10	16	4L7B	2.41
5	3VNH	2.10	17	4L7C	2.40
6	3ZGC	2.20	18	4L7D	2.25
7	3ZGD	1.98	19	4N1B	2.55
8	4CXI	2.35	20	4XMB	2.43
9	4CXJ	2.80	21	5DAD	2.61
10	4CXT	2.66	22	5DAF	2.37
11	4IFJ	1.80	23	5F72	1.85
12	4IFL	1.80	24	5X54	2.30

Table 3 RMSD$_{min}$ of 13 PDB files

Index	PDB ID	RMSD$_{min}$ (Å)
1	2FLU	0.81[a]
2	3VNG	2.75
3	3VNH	1.88
4	3ZGC	1.75
5	4IFL	0.83[a]
6	4IFN	0.44
7	4IN4	0.71
8	4IQK	1.00
9	4L7B	0.71
10	4L7C	0.80
11	4L7D	0.37
12	4N1B	0.48
13	4XMB	0.61

[a] ETGE motif was used to calculate RMSD values in 2FLU and 4IFL.

be used to compare docking precision (Table 3). The structure of the Keap1 Kelch domain bound to the Nrf2 16-mer peptide (PDB ID: 2FLU) was chosen after considering the ligand type, RMSD value, and resolution. The crystal structure of Keap1 in the 2FLU file was modified by adding hydrogen atoms and CHARMm force field[22,23] and used as a docking receptor. Three binding sites: site 1 (centre coordinates: x: −4, y: 6, z: 0, radius: 21 Å), site 2 (centre coordinates: x: 5, y: 9, z: 1, radius: 15 Å), and site 3 (centre coordinates: x: 7.36, y: 8.33, z: 1.77, radius: 15 Å) were selected according to the Kealp1 structure and receptor binding site. To perform molecular simulations, Discover Studio 2.5 for semi-flexible docking program CDOCKER was used.[22,24,25]

2.3. Fluorescence polarization assays

The assay was performed as described by Zhan et al.[26] with some modifications. Fluorescence polarization was analysed using a TECAN Infinite F200 Pro instrument (Tecan, Switzerland) for multifunctional enzyme analysis and black 384-well plates with non-binding surface (Corning, USA). Each well was filled with 40 μL containing 10 μL PBS, 10 μL of 4 mM small peptides, 10

μL of Keap1 Kelch domain at different concentrations, and 10 μL of 200 nM fluorescent probe.[27,28] The plates were covered and oscillated for 30 min at room temperature in the dark, and fluorescence polarization was measured at $\lambda_{ex} = 485$ nm and $\lambda_{em} = 535$ nm.[29] Based on the obtained values of fluorescence polarization, the dissociation constant (K_d) was calculated using the following equation:[26]

$$F_c = F_0 + \left(\frac{F_c - F_0}{C_{probe}}\right)\left(C_{probe} + 10^{[protein]} + K_d - \sqrt{\left(C_{probe} + 10^{[protein]} + K_d\right)^2 - 4C_{probe}10^{[protein]}}\right)$$

where F is fluorescence polarization, F_c is fluorescence polarization of the Keap1 Kelch domain-FITC-labelled 9-mer Nrf2 peptide complex, F_0 is fluorescence polarization of the FITC-labelled 9-mer Nrf2 peptide, C_{probe} is the final concentration of the FITC-labelled 9-mer Nrf2 peptide, and [protein] is the log$_{10}$ of Kelch domain final concentration.

2.4. Establishment of H$_2$O$_2$ damage model in HepG2 cells

HepG2 cells were seeded in culture dishes and grown in DMEM supplemented with 10% FBS, 1% PPS, and 1% non-essential amino acids. Cells were collected at 80–90% confluence, seeded into 96-well plates, and incubated for 12 h at 37 °C, 5% CO$_2$. Then, different concentrations of H$_2$O$_2$ were added to some wells (injury group), while the same amount of serum-free DMEM was added to the other wells (control group), and plates were incubated for 4 h at the same conditions.[30] Cell viability was analysed by adding 20 μL of MTS solution per 100 μL medium for 2 h and measuring the absorbance at 490 nm in a multi-mode microplate reader (Bio Tek Instruments, USA).[31]

2.5. Toxicity assay

HepG2 cells were seeded into 96-well plates for 12 h. Then, the test group received small peptides or the 9-merNrf2 peptide at different concentrations, while the control group received the same volume of serum-free DMEM.[31] After 2 h incubation, cell viability was analysed by the MTS assay as described above.[32]

2.6. Cytoprotection of H$_2$O$_2$-treated HepG2 cells by small peptides

The assay was performed according to Liu et al.[32] with some modifications. HepG2 cells were seeded into 96-well plates for 12 h and treated with different concentrations of small peptides (test group), 0.625 μM of the 9-mer Nrf2 peptide (positive control group), or serum-free DMEM (negative control group) for 2 h. Then, test wells and part of the control wells received 350 μM H$_2$O$_2$, while the other control wells received serum-free DMEM. After incubation for 4 h, cell viability was analysed as described above.[30]

2.7. Measurement of antioxidant enzyme activities

HepG2 cells were seeded into 96-well plates and incubated with small peptides, 0.625 μM of the 9-mer Nrf2 peptide, and 350 μM H$_2$O$_2$ as described above. Then, culture medium was removed,

and cells monolayers were rinsed twice with PBS and treated with cell lysis buffer for 30 min on ice.[32] The resulting cell lysates were centrifuged at 13 000 × g at 4 °C for 5 min, and total protein and CAT and SOD activities were measured using the corresponding assay kits.[31]

2.8. Statistical analysis

Fluorescence polarization assays and cell experiments were performed in triplicate, and the obtained data were expressed as the mean ± SEM. The difference between two groups was analysed by one-way ANOVA and considered significant at $p < 0.05$.

3. Results

3.1. Molecular docking

There were 24 PDB files related to human Keap1 protein in the RCSB database, but only 13 of them (PDB ID: 2FLU, 3VNG, 3VNH, 3ZGC, 4IFL, 4IFN, 4IN4, 4IQK, 4L7B, 4L7C, 4L7D, 4N1B, and 4XMB) included ligands that marked binding sites. The ligands and receptors from these files were docked by CDOCKER, and their $RMSD_{min}$ values were obtained (Table 3). Two of these PDB files (2FLU and 4IFL) used the ETGE motif to calculate the RMSD value, and the ligand in these files was the 16-mer Nrf2 peptide (H-AFFAQLQLDEETGEFL-OH, residues 69–84) with an unstable structure; therefore, the files were unsuitable for calculating the RMSD value by docking directly with their ligands and receptors. ETGE was the key motif of the 16-mer Nrf2 peptide, as it is critical for binding to the Keap1 Kelch domain;[34] therefore, it was used to calculate RMSD in 2FLU and 4IFL. It has been generally accepted that the $RMSD_{min}$ value less than 2.0 Å could be subjected to molecular docking experiments,[33] so 12 PDB files (PDB ID: 2FLU, 3VNH, 3ZGC, 4IFL, 4IFN, 4IN4, 4IQK, 4L7B, 4L7C, 4L7D, 4N1B, and 4XMB) could be used. Among them, only three (2FLU, 3ZGC, and 4IFL) contained Keap1 and ETGE (residues 79–82) of Nrf2, and could directly reveal Keap1–Nrf2 interaction,[34,35] whereas the ligands in the other PDB files were small non-peptide compounds (RCSB database; http://www.pdb.org). Therefore, the crystal structures of the Keap1 protein shown in 2FLU, 3ZGC, and 4IFL files were more suitable for investigating the interaction between Keap1 and its peptidomimetic inhibitor. However, the ligand in the 3ZGC file was a cyclic peptide that did not correspond to the native Nrf2; hence, it was not used in this study. The remaining 2FLU and 4IFL files contained the native Nrf2 as a ligand, but the resolution in 2FLU (1.50 Å) was higher than that in 4IFL (1.80 Å, Table 2) and the $RMSD_{min}$ (0.81 Å versus 0.83 Å, respectively) was lower (Table 3). Therefore, we chose 2FLU as the receptor file; in addition, 2FLU was frequently used in previous molecular docking experiments.[36–38]

The Keap1 Kelch domain had a central cavity[39] and bound Nrf2 through key amino acid residues located above this cavity (Fig. 2A1 and A2). Based on the central cavity structure, it was obvious that the binding of small peptides to the Keap1 Kelch domain varied depending on the site (Fig. 2B1–G1). The results of molecular docking were obtained using CDOCKER_ENERGY as an index: higher CDOCKER_ENERGY indicated stronger binding affinity of the tested small peptides to the Keap1 Kelch domain. The best six ligand poses identified by molecular docking of di-peptides to each site of the Keap1 Kelch domain were EK, DK, DW, EW, WE, and EY (Fig. 2B2–D2), although their binding affinity to different sites varied. The best 10 ligand poses identified by molecular docking of tri-peptides to each site of the Keap1 Kelch domain were DKE, QKE, DKD, EDW, DWE, DKK, EEW, EWE, ECD, DWD, DET, DEW, DDW, and DKQ (Fig. 2E2–G2). The CDOCKER_ENERGY values of the best ligand pose for di-peptides in sites 1, 2, and 3 were 49.23, 77.16, and 75.43 kcal mol^{-1}, respectively. The CDOCKER_ENERGY values of the best ligand pose for tri-peptides in sites 1, 2, and 3 were 71.89, 106.66, and 106.82 kcal mol^{-1}, respectively. These data indicate that the binding affinity of small peptides to site 1 of the Keap1 Kelch domain was significantly lower than that to sites 2 and 3, whereas there was no significant difference in peptide binding affinity to sites 2 and 3.

3.2. Fluorescence polarization assay

Competitive inhibition of Nrf2 binding to the Keap1 Kelch domain by 20 small peptides was analysed by the fluorescence polarization assay using the FITC-labelled 9-mer Nrf2 peptide containing the ETGE motif which exhibits 100 times higher binding affinity to the Kelch domain compared to that of another Kelch-binding motif, DLG. As evidenced by the K_d values (Fig. 3A) and binding curves (Fig. 3B), only two tri-peptides, DKK and DDW, could significantly decrease the binding of the FITC-labelled Nrf2 peptide to the Keap1 Kelch domain, indicating that these peptides specifically inhibited Nrf2 association with Keap1. These results suggested that the DKK and DDW peptides docked into the binding site for Nrf2 on the Keap1 Kelch domain, thus inhibiting Keap1–Nrf2 interaction.
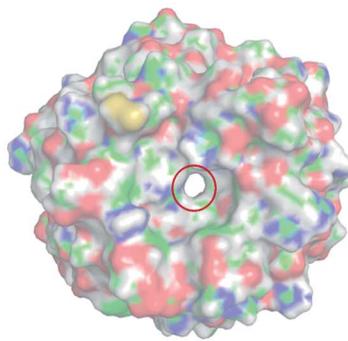
3.3. HepG2 cell model of oxidative damage, cytotoxicity, and cytoprotection

Next, the DKK and DDW tri-peptides selected based on the affinity to the Keap1 Kelch domain were tested for the ability to protect cells against oxidative stress. HepG2 cells were treated with H_2O_2, which decreased their survival in a concentration-dependent manner (Fig. 4A). As 350 μM H_2O_2 caused ∼50% inhibition of cell viability compared to that in untreated control ($p < 0.01$), this concentration was chosen to test the antioxidant effects of the selected tri-peptides.
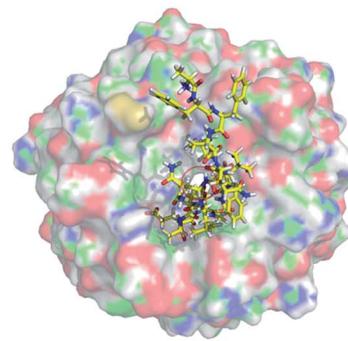
The DKK and DDW peptides were not cytotoxic at the concentration range from 0.1 μM to 100 μM, but decreased cell viability at 1000 μM compared to that in control ($p < 0.01$, Fig. 4B). At the same time, the 9-mer Nrf2 peptide was not cytotoxic at concentrations from 0.5 μM to 10 μM, but decreased cell viability at 20 μM compared to that in control ($p < 0.05$; Fig. 4B). The peptides at non-cytotoxic concentrations were examined for protective effects on H_2O_2-treated HepG2 cells, and the 9-mer Nrf2 peptide (0.625 μM) was chosen as positive control, because it has been shown to interfere with Keap1–Nrf2 interaction.[10] H_2O_2 at 350 μM significantly decreased cell viability compared to that in control ($p < 0.01$); however, the 9-mer Nrf2 peptide could significantly increase the viability of H_2O_2-treated HepG2 cells ($p < 0.05$,

Fig. 2 Ligand docking into the Keap1 Kelch domain. (A1) The structure of the Keap1 Kelch domain; (A2) binding of the 16-mer Nrf2 peptide (residues 69–84) to the Keap1 Kelch domain. (B–D) Interaction of di-peptides with the Keap1 Kelch domain in site 1 (B1), site 2 (C1), and site 3 (D1). The best six poses of molecular docking for di-peptides into site 1 (B2), site 2 (C2), and site 3 (D2). (E–G) Interaction of tri-peptides with the Keap1 Kelch domain in site 1 (E1), site 2 (F1), and site 3 (G1). The best 10 poses of molecular docking of tri-peptides into site 1 (E2), site 2 (F2), and site 3 (G2). R1, R2, and R3 represent peptide side-chain groups. The central cavity of the Keap1 Kelch domain is circled.

Result of interactions of Keap1 and di-peptides on site 1

Peptide	-CDOCKER_ENERGY (kcal/mol)	Origin
EK	49.23	Ovalbumin, Ovotransferrin, etc.
DK	47.20	Ovalbumin, Ovotransferrin, etc.
WE	43.87	Ovalbumin, Ovotransferrin, etc.
DW	41.75	Ovotransferrin, Ovomucin, etc.
EY	40.04	Ovalbumin, Ovotransferrin, etc.
EW	38.96	Ovalbumin, Ovotransferrin, etc.

Result of interactions of Keap1 and di-peptides on site 2

Peptide	-CDOCKER_ENERGY (kcal/mol)	Origin
EY	77.16	Ovalbumin, Ovotransferrin, etc.
DK	76.72	Ovalbumin, Ovotransferrin, etc.
EK	74.31	Ovalbumin, Ovotransferrin, etc.
EW	72.56	Ovalbumin, Ovotransferrin, etc.
DW	71.36	Ovotransferrin, Ovomucin, etc.
WE	69.75	Ovalbumin, Ovotransferrin, etc.

Result of interactions of Keap1 and di-peptides on site 3

Peptide	-CDOCKER_ENERGY (kcal/mol)	Origin
EY	75.43	Ovalbumin, Ovotransferrin, etc.
DK	74.56	Ovalbumin, Ovotransferrin, etc.
EW	74.03	Ovalbumin, Ovotransferrin, etc.
EK	73.85	Ovalbumin, Ovotransferrin, etc.
DW	70.83	Ovotransferrin, Ovomucin, etc.
WE	68.77	Ovalbumin, Ovotransferrin, etc.
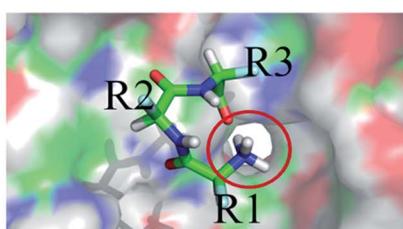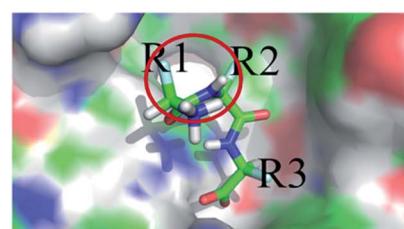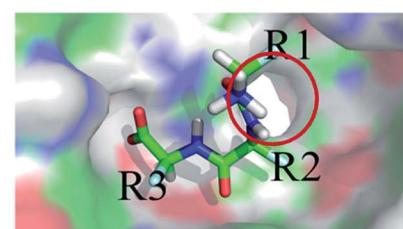
Result of interactions of Keap1 and tri-peptides on site 1

Peptide	-CDOCKER_ENERGY (kcal/mol)	Origin
DKE	71.89	Ovomucoid, Ovomucin, etc.
QKE	67.37	Avidin, etc.
DKD	66.82	Lipovitellin-1(Vitellogenin-1), etc.
EDW	66.02	Alpha-actinin-1, etc.
DWE	63.36	Riboflavin-binding protein, etc.
DKK	62.35	Ovomucin, etc.
EEW	62.09	Alpha-actinin-1, etc.
EWE	61.52	Ovotransferrin, etc.
ECD	61.18	Ovomucin, etc.
DWD	60.75	Alpha-actinin-1, etc.

Result of interactions of Keap1 and tri-peptides on site 2

Peptide	-CDOCKER_ENERGY (kcal/mol)	Origin
DWE	106.66	Riboflavin-binding protein, etc.
EWE	104.83	Ovotransferrin, etc.
EEW	103.58	Alpha-actinin-1, etc.
DET	103.11	Ovotransferrin, Ovomucin, etc.
DKE	102.70	Ovomucoid, Ovomucin, etc.
DWD	101.96	Alpha-actinin-1, etc.
EDW	100.92	Alpha-actinin-1, etc.
DEW	100.67	Protein AATF, etc.
DKD	100.56	Lipovitellin-1(Vitellogenin-1), etc.
DDW	98.96	Avidin, etc.

Result of interactions of Keap1 and tri-peptides on site 3

Peptide	-CDOCKER_ENERGY (kcal/mol)	Origin
DWE	106.82	Riboflavin-binding protein, etc.
DKD	106.62	Lipovitellin-1(Vitellogenin-1), etc.
DET	105.82	Ovotransferrin,Ovomucin, etc.
EWE	105.69	Ovotransferrin, etc.
DKE	105.15	Ovomucoid,Ovomucin, etc.
EEW	104.87	Alpha-actinin-1, etc.
DWD	101.72	Alpha-actinin-1, etc.
EDW	100.73	Alpha-actinin-1, etc.
DEW	99.76	Protein AATF, etc.
DKQ	98.43	YGP40, etc.

Fig. 4C). Although the protective effect of the DKK and DDW peptides at low concentrations (0.1 μM and 1.0 μM) was not statistically significant, at high concentrations (10.0 μM and 100.0 μM), DKK and DDW could significantly increase the viability of H_2O_2-treated HepG2 cells ($p < 0.05$ and $p < 0.01$, respectively,

Fig. 4C). Furthermore, DKK (100.0 μM) and DDW(10.0 μM and 100.0 μM) showed a significantly higher protective effect compared to the 9-mer Nrf2 ($p < 0.05$ and $p < 0.01$, respectively). These results suggest that tri-peptides DKK and DDW can protect HepG2 cells from oxidative stress.

A
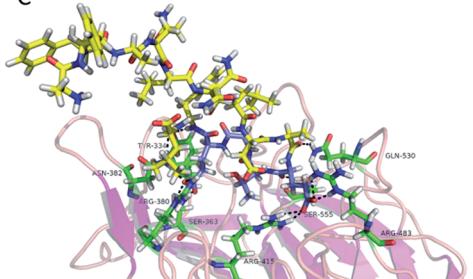
Inhibition of the Keap1 Kelch domain interaction with Nrf2 by short egg-derived peptides

Group	peptides	K_d (nM)
Control group	-	21.99 ± 6.02
Test group	DKE	16.13 ± 5.20
Test group	EWE	24.26 ± 7.66
Test group	EEW	31.83 ± 11.35
Test group	EDW	15.65 ± 4.82
Test group	DWE	11.63 ± 4.14
Test group	DKD	23.44 ± 7.27
Test group	QKE	20.57 ± 4.98
Test group	ECD	24.73 ± 3.79
Test group	DET	18.89 ± 2.04
Test group	DKQ	22.70 ± 2.80
Test group	DWD	11.58 ± 2.13
Test group	DEW	19.44 ± 2.50
Test group	EK	18.70 ± 5.26
Test group	DW	12.19 ± 3.78
Test group	WE	11.55 ± 5.03
Test group	EW	32.0 ± 17.39
Test group	EY	6.86 ± 1.89
Test group	DK	8.61 ± 3.24
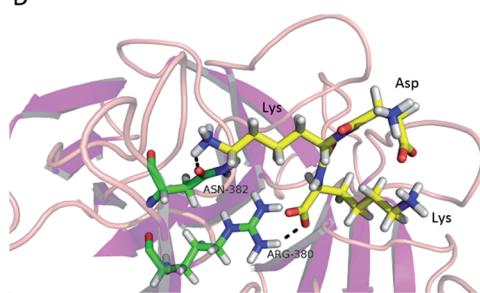
B

C

D

E
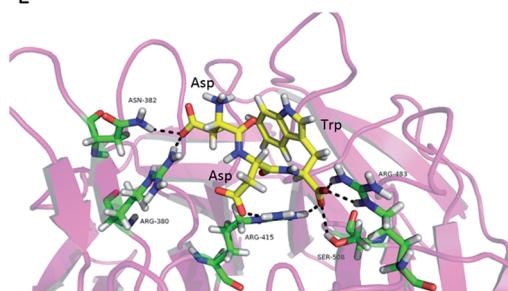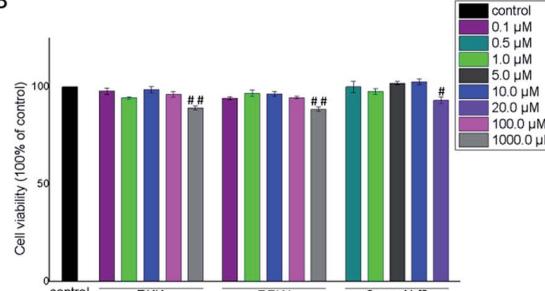
Fig. 3   Inhibition of the Keap1 Kelch domain interaction with Nrf2 by short egg-derived peptides. (A, B) Competitive inhibition of Keap1 Kelch binding to FITC-labelled 9-mer Nrf2 by egg-derived peptides was analysed by the fluorescence polarization assay. Fluorescence polarization was measured at $\lambda_{ex} = 485$ nm and $\lambda_{em} = 535$ nm, and K_d values are shown as the mean ± SEM. (C–E) Interaction of 16-mer Nrf2 (C), DKK (D), and DWW (E) peptides with the residues of the Keap1 Kelch domain.

A
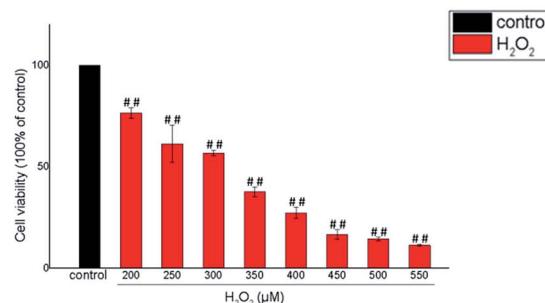
B

C
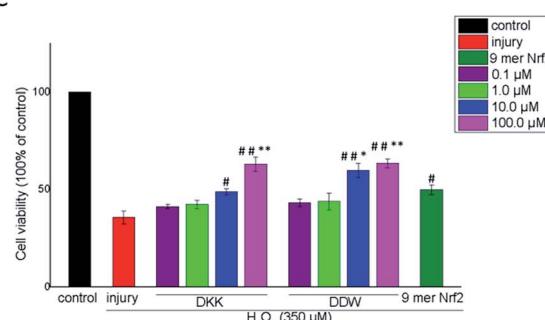
Fig. 4   Protection of H_2O_2-treated HepG2 cells by the DKK and DDW peptides. (A) Cytotoxicity of H_2O_2. HepG2 cells were treated with the indicated concentrations of H_2O_2 for 4 h at 37 °C. (B) Cytotoxicity of DKK and DDW. HepG2 cells treated with the indicated concentrations of the peptides for 2 h at 37 °C. (C) Protection of H_2O_2-treated HepG2 cells by DKK and DDW. Cells were first treated with the indicated concentrations of DKK and DDK for 2 h, and then with 350 μM H_2O_2 for 4 h. Cell viability was evaluated by the MTS assay. The data are presented as the mean ± SEM; $^{\#}p < 0.05$, $^{\#\#}p < 0.01$ compared to control (A, B) or H_2O_2 treatment (C), and $^{*}p < 0.05$, $^{**}p < 0.01$ compared to the 9-mer Nrf2 peptide at 0.625 μM (C).

3.4.   Antioxidant enzyme activity

To further investigate the antioxidant potential of the tri-peptides, we measured the activity of CAT and SOD, the enzymes involved in detoxification of reactive oxygen species (ROS). The results indicate that H_2O_2 downregulated CAT in HepG2 cells and that the 9-mer Nrf2 peptide could increase CAT and SOD activity in H_2O_2-treated cells, although the effect was

A

B

C
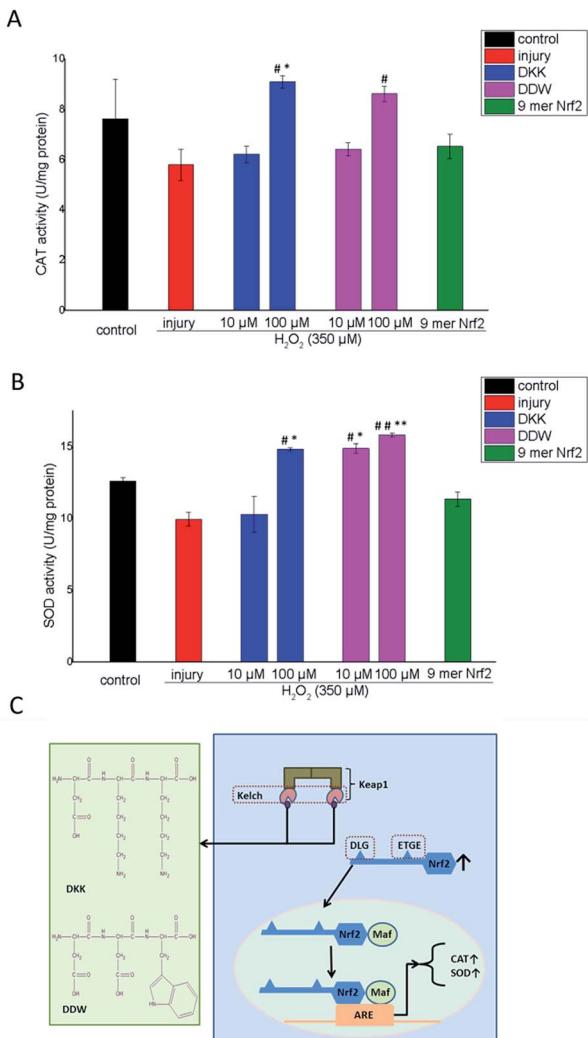
Fig. 5 Effects of the DKK and DDW peptides on CAT and SOD activity in H_2O_2-treated HepG2 cells. Cells were treated with the indicated concentrations of DKK or DDK for 2 h, and then with 350 μM H_2O_2 for 4 h at 37 °C. (A) CAT and (B) SOD enzymatic activities were measured using commercial assay kits. The data are presented as the mean ± SEM; $^{#}p < 0.05$, $^{##}p < 0.01$ compared to H_2O_2 treatment, and $^{*}p < 0.05$, $^{**}p < 0.01$ compared to the 9-mer Nrf2 peptide (0.625 μM). (C) Schematic illustration of the putative mechanism underlying DKK and DDW effects on the expression of CAT and SOD.

not statistically significant. The reason why Nrf2 could improve cell viability but not the activity of CAT and SOD may be that it could bind its targets on the cell surface but was too large to penetrate cells and activate the Keap1–Nrf2 pathway in order to increase CAT and SOD activities. However, DKK and DDW increased CAT activity in H_2O_2-treated cells in a concentration-dependent manner, and the effect was statistically significant at 100 μM ($p < 0.05$ compared to H_2O_2 alone and 9-mer Nrf2; Fig. 5A). Similarly, the activity of SOD decreased by H_2O_2 treatment was rescued by the addition of tri-peptides at 10 μM and 100 μM (Fig. 5B). While the effect of the DKK peptide on SOD activity was statistically significant only at high concentration (100 μM; $p < 0.05$ compared to H_2O_2 alone and 9-mer Nrf2), DDW could upregulate SOD both at low (10 μM; $p < 0.05$)

and high (100 μM; $p < 0.01$) concentrations compared to H_2O_2 alone and 9-mer Nrf2 (Fig. 5B).

4. Discussion

Eggs are a rich source of proteins, and various small peptides with antioxidant activity can be obtained from eggs through protein degradation. Among the antioxidant pathways, Keap1–Nrf2 signalling is one of the most important in the oxidation process.[10] Although a number of methods have been applied to study direct inhibitory effects of small molecules on Keap1–Nrf2 interaction, most of them are complicated and not suitable for high throughput screening.[40] Molecular docking is a rapid and cost-effective method based on simulating molecular interactions, which could be applied for high throughput screening of small target molecules.[22–25,40] Therefore, we used the molecular docking approach for preliminary screening of egg-derived peptides for the affinity to Keap1 and ability to inhibit Keap1–Nrf2 binding. The structure of the Keap1:Nrf2 interface (PDB ID: 2FLU), representing the human Keap1 Kelch domain bound to a 16-mer Nrf2 peptide was used here for modelling Keap1–Nrf2 interactions. The 16-mer Nrf2 peptide binds to Keap1 mainly through hydrogen bonding with the six amino-acid stretch(78-EETGEF-83) which has a size significantly exceeding that of the tested di- and tri-peptides (Fig. 2A2), indicating that the peptides could only partially occupy the Keap1 binding site for Nrf2. Therefore, we could not use this site in the docking experiments with our small peptides. To reduce the impact of size difference and increase the accuracy of the analysis, the following three binding sites were designed. Site 1 was obtained based on the Keap1 binding site for 16-mer Nrf2 peptide; site 2 was designed based on all Keap1 amino acids positioned within 3.5 Å from the 16-mer Nrf2 peptide; finally, site 3 was based on the ETGE motif in the 16-mer Nrf2 peptide. Then, a ligand library of short egg-derived peptides was screened and 14 tri- and six di-peptides were selected according to their potential to directly interfere with the binding of Keap1 to Nrf2, as predicted by molecular docking.

These candidate peptides were tested in the fluorescence polarization assay, which is an effective method to detect molecular interactions in a non-cellular environment, because it is rapid and generates reproducible data.[26–28] In the competitive fluorescence polarization test, IC_{50} is commonly used as an index to evaluate the binding affinity of a ligand to the receptor. However, according to Inoyama et al.,[28] the IC_{50} value could not reflect the binding affinity between Keap1 and peptides shorter than seven amino acids, i.e., the di- and tri-peptides tested in our study. Therefore, we used K_d rather than IC_{50} as an evaluation index in the fluorescence polarization assay, because it had higher detection sensitivity compared to IC_{50}. Among the 20 small peptides tested, two tri-peptides, DKK and DDW, could significantly inhibit Keap1–Nrf2 binding as evidenced by the increase in the K_d value (Fig. 3B). Our analysis indicates that DKK and DDW form hydrogen bonds with the residues in the Keap1 Kelch domain involved in Keap1–Nrf2 interaction. Thus, DKK binds to Arg380 and Asn382 (Fig. 3D), while DDW binds to Arg380, Asn382, Arg415, Arg483, and Ser508 (Fig. 3E), which are

key residues in the binding site for the 16-mer Nrf2 peptide in the Keap1 Kelch domain (Tyr343, Ser363, Arg380, Asn382, Arg415, Arg483, Gln530, and Ser555) (Fig. 3C).[33] Hence, DKK and DDW occupy the binding site for Nrf2 in the Kelch domain and prevent the Keap1–Nrf2 interaction, which may result in the induction of cellular antioxidant mechanisms.

Indeed, our findings indicate that the DKK and DDW peptides could protect HepG2 cells against H_2O_2-induced damage, increasing their viability and upregulating the activity of key antioxidant enzymes CAT and SOD. The putative mechanism underlying the protective effects of the tripeptides against oxidative stress is shown in Fig. 5C. The DKK and DDW peptides partially occupy the Keap1 binding site for Nrf2 through hydrogen bonding with the key residues, thus preventing the proteasomal degradation of Nrf2. The accumulated Nrf2 then translocates to the nucleus, where it forms heterodimers with the Maf protein and binds to Antioxidant Response Element (ARE), activating gene expression of phase II detoxification enzymes, including CAT and SOD.[10,17,18] Further studies in cellular models are required to confirm this mechanism. Considering that the selected tripeptides are not cytotoxic at the concentrations providing cell protection against oxidative stress, they can be also tested in experimental animals.

5. Conclusions

Our study indicates that the combination of molecular docking and fluorescence polarization methods can be applied to effective screening of direct Nrf2 inhibitors. As a result, small egg-derived peptides DKK and DDW were identified as direct inhibitors of the Keap1–Nrf2 interaction, which could improve cell resistance to oxidative stress, suggesting their potential as antioxidants.

Abbreviations

Nrf2	Nuclear factor erythroid 2-related factor 2
Keap1	Kelch-like ECH-associated protein 1
HO-1	Hemeoxygenase 1
NQO1	NAD(P)H dehydrogenase 1
SOD	Superoxide dismutase
CAT	Catalase
Maf	Musculoaponeurotic fibrosarcoma
ARE	Antioxidant response element

Acknowledgements

References

1 L. Ding, Y. Zhang, Y. Q. Jiang, L. Y. Wang, B. Q. Liu and J. B. Liu, *J. Agric. Food Chem.*, 2014, **62**, 3177–3182.
2 J. B. Liu, Z. P. Yu, W. Z. Zhao, S. Y. Lin, E. L. Wang and Y. Zhang, *Food Chem.*, 2010, **122**, 1159–1163.
3 Z. P. Yu, W. Z. Zhao, J. B. Liu, J. Lu and Z. F. Chen, *J. Sci. Food Agric.*, 2011, **91**, 921–926.
4 C. Chen, Y. J. Chi, M. Y. Zhao and L. Lv, *Amino Acids*, 2012, **43**, 457–466.
5 O. K. Chang, G. E. Ha, G. S. Han, K. H. Seol, H. W. Kim, S. G. Jeong, M. H. Oh, B. Y. Park and J. S. Ham, *J. Agric. Food Chem.*, 2013, **61**, 7294–7300.
6 S. Shen, B. Chahal, K. Majumder, S. J. You and J. P. Wu, *J. Agric. Food Chem.*, 2010, **58**, 7664–7672.
7 M. Brandsch, I. Knuetter and E. Bosse-Doenecke, *J. Pharm. Pharmacol.*, 2008, **60**, 543–585.
8 B. S. Vig, T. R. Stouch, J. K. Timoszyk, Y. Quan, D. A. Wall, R. L. Smith and T. N. Faria, *J. Med. Chem.*, 2006, **49**, 3636–3644.
9 X. M. Wang, H. X. Chen, X. G. Fu, S. Q. Li and J. Wei, *LWT–Food Sci. Technol.*, 2017, **75**, 93–99.
10 S. Magesh, Y. Chen and L. Q. Hu, *Med. Res. Rev.*, 2012, **32**, 687–726.
11 L. Baird and A. T. Dinkova-Kostova, *Arch. Toxicol.*, 2011, **85**, 241–272.
12 D. D. Zhang, *Antioxid. Redox Signaling*, 2010, **13**, 1623–1626.
13 D. D. Zhang, S. C. Lo, Z. Sun, G. M. Habib, M. W. Lieberman and M. Hannink, *J. Biol. Chem.*, 2005, **280**, 30091–30099.
14 F. Hong, K. R. Sekhar, M. L. Freeman and D. C. Liebler, Specific patterns of electrophile adduction trigger Keap1 ubiquitination and Nrf2 activation, *J. Biol. Chem.*, 2005, **280**, 31768–31775.
15 M. McMahon, N. Thomas, K. Itoh, M. Yamamoto and J. D. Hayes, *J. Biol. Chem.*, 2006, **281**, 24756–24768.
16 D. D. Zhang and M. Hannink, *Mol. Cell. Biol.*, 2003, **23**, 8137–8151.
17 A. Kobayashi, M. I. Kang, Y. Watai, K. I. Tong, T. Shibata, K. Uchida and M. Yamamoto, *Mol. Cell. Biol.*, 2006, **26**, 221–229.
18 A. Uruno and H. Motohashi, *Nitric Oxide*, 2011, **25**, 153–160.
19 X. J. Wang, Z. Sun, W. Chen, Y. Li, N. F. Villeneuve and D. D. Zhang, *Toxicol. Appl. Pharmacol.*, 2008, **230**, 383–389.
20 S. J. Chapple, R. C. M. Siow and G. E. Mann, *Int. J. Biochem. Cell Biol.*, 2012, **44**, 1315–1320.
21 J. T. Kern, M. Hannink and J. F. Hess, *Curr. Top. Med. Chem.*, 2007, **7**, 972–978.
22 T. Onoda, W. Li, T. Sasaki, M. Miyake, K. J. Higai and K. Koike, *J. Ethnopharmacol.*, 2016, **186**, 84–90.
23 D. Wu, J. Yan, J. Wang, Q. Wang and W. Li, *Food Chem.*, 2015, **170**, 423–429.
24 G. K. Panigrahi, M. K. Suthar, N. Verma, S. Asthana, A. Tripathi, S. K. Gupta, J. K. Saxena, S. Raisuddin and M. Das, *Food Res. Int.*, 2015, **77**, 368–377.
25 A. Singh, S. K. Paliwal, M. Sharma, A. Mittal, S. Sharma and J. P. Sharma, *J. Mol. Graphics Modell.*, 2016, **63**, 1–7.

26 C. Y. Zhan, K. Varney, W. R. Yuan, L. Zhao and W. Y. Lu, *J. Am. Chem. Soc.*, 2012, **134**, 6855–6864.

27 Z. Y. Jiang, M. C. Lu, L. L. Xu, T. T. Yang, M. Y. Xi, X. L. Xu, X. K. Guo, X. J. Zhang, Q. D. You and H. P. Sun, *J. Med. Chem.*, 2014, **57**, 2736–2745.

28 D. Inoyama, Y. Chen, X. Y. Huang, L. J. Beamer, T. A. N. Kong and L. Q. Hu, *J. Biomol. Screening*, 2012, **17**, 435–447.

29 R. Hancock, H. C. Bertrand, T. Tsujita, S. Naz, A. El-Bakry, J. Laoruchupong, J. D. Hayes and G. Wells, *Free Radical Biol. Med.*, 2012, **52**, 444–451.

30 J. B. Liu, Z. F. Chen, J. He, Y. Zhang and T. Zhang, *Food Funct.*, 2014, **5**, 3179–3188.

31 E. Kerasioti, D. Stagos, A. Tzimi and D. Kouretas, *Food Chem. Toxicol.*, 2016, **97**, 47–56.

32 D. Liu, F. G. Pan, J. Y. Liu, Y. Wang, T. Zhang, E. L. Wang and J. B. Liu, *RSC Adv.*, 2016, **6**, 81092–81100.

33 H. Gohlke, M. Hendlich and G. Klebe, *J. Mol. Biol.*, 2000, **295**, 337–356.

34 S. C. Lo, X. C. Li, M. T. Henzl, L. J. Beamer and M. Hannink, *EMBO J.*, 2006, **25**, 3605–3617.

35 S. Hörer, D. Reinert, K. Ostmann, Y. Hoevels and H. Nar, *Acta Crystallogr.*, 2013, **69**, 592–596.

36 S. Mikiya, S. Hajime, T. Tomoyuki, M. Yoshinori, N. Hisashi, S. Rieko, Y. Naoyoshi, I. Hideki, N. Noriko, Y. Yoshitaka, A. Takumi, T. Ryuji and K. Naoki, *FEBS Open Bio*, 2015, **5**, 557–570.

37 B. Elango, D. Kesavan, K. Suresh, S. Dornadula, H. Waheeta, P. Ramasamy and R. M. Kunka, *Bioorg. Med. Chem.*, 2016, **24**, 3378–3386.

38 N. C. Andreia, M. Carla, C. G. Rita, C. C. Margarida, R. Elsa, V. H. Jack and J. G. Maria, *FEBS Lett.*, 2016, **590**, 1455–1466.

39 B. Padmanabhan, K. I. Tong, T. Ohta, Y. Nakamura, M. Scharlock, M. Ohtsuji, M. Kang, A. Kobayashi, S. Yokoyama and M. Yamamoto, *Mol. Cells*, 2006, **21**, 689–700.

40 B. C. Pearce, D. R. Langley, J. Kang, H. W. Huang and A. Kulkarni, *J. Chem. Inf. Model.*, 2009, **49**, 1797–1809.